CONTRIBUTIONS TO THE INVESTIGATIONS OF CLASSICAL OPTICS–BALLISTIC ELECTRONS ANALOGIES

Daniela DRAGOMAN[1]

Reception speech at the Academy of Romanian Scientists, January 30, 2024

It is with emotion and gratitude to those who made this moment possible that I deliver this traditional reception speech. It was quite difficult for me to choose the topic of this speech since during my scientific activity I investigated a quite wide range of domains of interest, which include: (i) phase space studies of optics and quantum physics, regarding especially the evolution of light beams and quantum wavefunctions, as well as the development of a phase space formalism of quantum mechanics, (ii) modeling of ballistic nanostructures and extending their applications in nanoelectronics, reversible logic, high-frequency devices, etc., (iii) quantum–classical analogies, encompassing classical optics–ballistic electrons analogies and classical–quantum optics analogies, and, not least, (iv) nanophotonics, in particular plasmonics, metasurfaces and optical vortices. After some consideration, finally I have decided to present in front of you some contributions to the subject of classical optics–ballistic electrons analogies.

DOI **10.56082/annalsarsciphyschem.2024.1.64**

1. Introduction

The subject of this reception speech is one of the most interesting research topics that I dealt with, at the same productive from the point of view of the results obtained and still of relevance, namely the analogies between classical optics and ballistic electrons, which propagate coherently and are described by the same quantum wavefunction. After a short introduction in the topic, I will focus on some personal contributions to the development of this subject.

At a first glance, to emphasize analogies between domains of physics that are so different can be surprising. Indeed, ballistic electrons, i.e., those that do not suffer

[1]Prof., PhD, Faculty of Physics, University of Bucharest, full member of the Academy of Romanian Scientists, (e-mail: daniela@solid.fizica.unibuc.ro).

collisions during propagation, irrespective if described by the Schrödinger or Dirac equations, and classical light beams that satisfy Maxwell's equations differ not only from the point of view of the evolutive equations but also in terms of quantum statistics (electrons being fermions that obey the Pauli exclusion principle and having half-integer spin whereas photons are bosons which do not obey the Pauli principle and have integer spin), charge (electrons being negatively charged with the elementary charge e whereas photons are electrically neutral), wavefunction type (scalar for electrons that satisfy the Schrödinger equation, vectorial for the electromagnetic field, or spinorial for electrons obeying the Dirac equation), and dispersion relation, respectively, effective mass. The dispersion relation is parabolic for electrons satisfying the Schrödinger equation, which have a finite effective mass, and linear for photons and Dirac electrons in graphene, characterized by zero effective mass. However, analogies have provided for a long time and still offer in the present the opportunity to look at certain problems from nonconformal points of view, which led to respectively have the potential to initiate the development of new research avenues in physics. This is the reason why analogies between different domains in physics deserve to be investigated.

2. Classical optics–ballistic electrons analogies based on the similarity of evolution equations

In one of the first applications, the analogies between classical optics and ballistic electrons that satisfy the Schrödinger equation allowed the construction of the optical microscope [1], for which Ernst Ruska was awarded with the Nobel Prize in Physics in 1986. In this case, the ballistic electrons propagate in vacuum, the time-independent Schrödinger equation that these obey,

$$-\frac{\hbar^2}{2m}\nabla^2\Psi + (V-E)\Psi = 0 \tag{1}$$

being similar to the Helmholtz equation

$$\nabla^2\boldsymbol{A} + k^2\boldsymbol{A} = 0 \tag{2}$$

satisfied, for instance, by the vector potential $\boldsymbol{A}$ of the monochromatic electromagnetic field. Equations (1) and (2) are mathematically similar if

(i) $\boldsymbol{A}$ is equivalent with the wavefunction Ψ,

and

(ii) $k = \omega\sqrt{\varepsilon\mu} = \omega n/c$ is equivalent to $[2m(E-V)]^{1/2}/\hbar = [2mE_{kin}]^{1/2}/\hbar$.

In these expressions m is the effective mass of electrons with energy E that propagate in a region with potential energy V, E_{kin} is their kinetic energy and ω is

the frequency of electromagnetic radiation propagating with wavenumber k in a medium with electric permittivity ε and magnetic permeability μ, whilst c is the light speed in vacuum.

While the classical optics-ballistic electrons analogies were originally applied to electrons propagating in vacuum, with the advancement of nanotechnologies it became evident that ballistic electrons can be encountered also in nanostructures with dimensions along one, two or three directions in space smaller than the average distance between two collisions, respectively in quantum wells, wires or dots. In these nanostructures, as suggested by the formal analogies mentioned above, a variation of the refractive index in an optical analog has the same effect on the electromagnetic field as the variation of the potential energy on the electron wavefunction [2,3]. In particular, at the interface between two media with different refractive indices, n_1 and n_2, the electromagnetic field satisfies the Snell law, which has a similar form for electrons propagating ballistically through the interface between two regions in which their kinetic energies take values E_{kin1} and E_{kin2}:

$$\sin\theta_1 / \sin\theta_2 = n_2/n_1 = \sqrt{E_{kin2}/E_{kin1}} \tag{3}$$

In the equation above θ_1 and θ_2 are the angles of the optical or electron beam with the normal at the interface between the two media.

Starting from these considerations, devices that illustrate the so-called "electron optics" were fabricated in nanostructures in which Schrödinger electrons propagate in a ballistic regime in quantum wells formed in two-dimensional electron gases. These are similar devices to those encountered in classical optics, e.g. electron prisms [4] or lenses [5] and even more complex devices such as Mach-Zehnder interferometers [6]. In this case, the propagation direction of electron beams, as well as their kinetic energy, can be varied using voltages applied on gate electrodes.

It should be mentioned in this context that the analogy works also in the opposite sense, the photonic crystals in optics, with allowed and forbidden frequency bands, being developed as analogs of crystalline materials [7], while the random lasers [8] were inspired by the phenomenon of weak localization [9] encountered in nanostructures. These lasers do not require a resonant cavity in order to generate coherent radiation, the active medium assuring both the amplification and the scattering and localization of the electromagnetic field.

Similarly, the Snell law in optics has an analog of the form

$$\sin\theta_1 / \sin\theta_2 = n_2/n_1 = (E - V_2)/(E - V_1) \tag{4}$$

for electrons with energy E that satisfy a Dirac-type equation in graphene and which traverse the interface between regions with potential energies V_1 and V_2. This is a consequence of the fact that the time-independent Dirac equation

$$\hbar v_F \begin{pmatrix} 0 & -i\frac{\partial}{\partial x} - \frac{\partial}{\partial y} \\ -i\frac{\partial}{\partial x} + \frac{\partial}{\partial y} & 0 \end{pmatrix} \begin{pmatrix} \Psi_1 \\ \Psi_2 \end{pmatrix} = (E - V) \begin{pmatrix} \Psi_1 \\ \Psi_2 \end{pmatrix} \quad (5)$$

with a spinorial wavefunction, can be expressed as

$$\left[\hbar^2 v_F^2 \left(\frac{\partial^2}{\partial x^2} + \frac{\partial^2}{\partial y^2}\right) + (E - V)^2\right] \Psi_{1,2} = 0 \quad (6)$$

for each of the two components of the spinor, Ψ_1 or Ψ_2. Equation (6) is similar to (2) as

(i) the vector potential $\boldsymbol{A}$ can be associated to one component of the spinorial wavefunction,

and

(ii) $k = \omega\sqrt{\varepsilon\mu} = \omega n/c$ can be put into correspondence with $(E - V)\ /\hbar v_F$.

Unlike for Schrödinger electrons, for Dirac electrons the Snell law in (4) holds for cases where the refractive index and, respectively, $E - V$, take negative values.

The existence of electrons satisfying a Dirac-type equation in a nonrelativistic regime was demonstrated for the first time in graphene [10], a two-dimensional material in which the carbon atoms form a hexagonal crystalline lattice. In graphene, the charge carriers have a linear dispersion relation around the non-equivalent K and K' corners of the first Brillouin zone, also of hexagonal form, corners that are called Dirac points. The two cones associated to the dispersion relations for electrons and holes in graphene touch in the Dirac points, this material having no bandgap.

The classical optics–ballistic electrons analogy made possible, also in graphene, the development of electrostatic [11] or magnetic [12] electron lenses and the experimental demonstration of interferential devices equivalent to a succession of coupled optical cavities [13]. In this situation, again, the modulation of the potential energy can be obtained by applying positive or negative voltages on gate electrodes, which shift the Fermi level above or, respectively, below the Dirac points, involving electrons or, respectively, hole states in the charge transport.

Once more, the specific characteristic of graphene, namely the existence of the linear dispersion relation around the Dirac points was observed also in two-dimensional photonic crystals in optics [14] with an arrangement of regions with different refractive indices similar to the hexagonal lattice of carbon atoms in

graphene. Recently, Dirac cones were observed also in two-dimensional photonic crystals with other symmetries [15].

These examples of the existing analogies and of their consequences on the development of new research directions in optics or nanoelectronics demonstrate the maturity of the analogy as investigating tool in physics. This method is still used, studies that extend the existing analogies being constantly published. An example in this respect is the application of the classical optics–Schrödinger electrons analogy to anisotropic systems, in particular for identifying a quantum analog of amphoteric refraction. This phenomenon is encountered in optics in uniaxial or biaxial birefringent crystals, and refers to the propagation of the transmitted wavevector (normal to the wavefront) and the Poynting vector at angles of opposite signs with respect to the normal at the interface between an isotropic and an anisotropic medium, which determines the energy transport direction. The amphoteric refraction in optics occurs in relatively narrow ranges of incidence angles only if the optical axis of the birefringent crystal is tilted with respect to the interface [16]. A similar phenomenon was predicted for electrons propagating in the ballistic regime in a two-dimensional electron gas at the interface between Bi_2Se_3 (isotropic medium) and Bi_2Te_3 (anisotropic crystal, with the principal axes of the energy/effective mass ellipsoid at an angle of 35° with respect to the crystalline axes [17]). Figure 1 illustrates the amphoteric refraction for electrons, $\boldsymbol{k}_1$, $\boldsymbol{k}_2$ representing the wavevectors of electrons that satisfy the Snell equation (3), $\boldsymbol{j}_1 = i(\hbar/2m_1)\,(\Psi\nabla\Psi^* - \Psi^*\nabla\Psi)$ is the current density probability in the isotropic medium and $\boldsymbol{j}_2$ the corresponding quantity in the anisotropic material. Amphoteric refraction for electrons occurs in wide ranges of the incidence angle (up to 80°), which depend also on the electron energy E, if the optical axis of the effective mass ellipsoid is tilted with respect to the interface [18]. In particular, for a dispersion relation in the anisotropic medium of the form $E - V_2 = \hbar^2(\alpha k_{2x}^2 + \beta k_y^2 + \gamma k_{2x}k_y)$, $\boldsymbol{k}_2$ propagates at the angle $\theta_2 = \arctan(k_y/k_{2x})$ and $\boldsymbol{j}_2$ at $\phi_2 = \arctan[(2\beta k_y + \gamma k_{2x})/(\gamma k_y + 2\alpha k_{2x})]$.

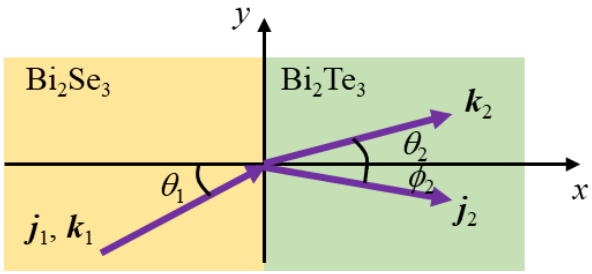

Fig. 1. Schematic representation of amphoteric refraction of ballistic electrons at an interface between an isotropic and an anisotropic material

Due to amphoteric refraction, an incident divergent electron beam normal to the Bi_2Se_3/Bi_2Te_3 interface is transformed into a steered beam, which propagates at a finite angle with respect to the normal at the interface that depends weakly on the energy of incident electrons, and has a much smaller angular divergence that varies with *E*.

Regarding the analogy between classical optics and electrons satisfying the Dirac equation in graphene, this was investigated especially for designing electron optics systems based on the Snell law in (4). A more detailed study of this subject is difficult, although photons and Dirac electrons share the same linear dispersion relation, because of the different characteristics of the electromagnetic field (vector) and quantum wavefunction (spinorial). Indeed, in classical optics a similar evolution equation to (5) is encountered in isotropic, gyrotropic and electro-optic media:

$$-i\frac{\lambda}{\pi}\frac{d}{dz}\begin{pmatrix}E_x\\E_y\end{pmatrix}=\begin{pmatrix}0 & \beta+i\gamma\\ \beta-i\gamma & 0\end{pmatrix}\begin{pmatrix}E_x\\E_y\end{pmatrix} \tag{7}$$

$E_{x,y}$ denoting the components of the electric field on the *x*,*y* directions in the transverse plane, while β and γ are the electro-optic and, respectively, gyrotropic coefficients. An example of such a material is $AgGaSe_2$, although a succession of thin layers of gyrotropic (magneto-optic, for example $(Bi,Sb)_2Te_3$) and electro-optic (for example, GaAs) materials can be used for implementing a medium with the mentioned properties. In this case, a formal analogy with (5) implies the equivalence between the following parameters:
(i) $z \leftrightarrow t$, $2\lambda \leftrightarrow \hbar$, $\beta \leftrightarrow k_x$, $\gamma \leftrightarrow -k_y$,

and, respectively, between

(ii) the Jones polarization vector, defined as $J^T = (E_x, E_y)^T$ and the spinorial wavefunction $\Psi^T = (\Psi_1, \Psi_2)^T$.

These equivalences could apparently suggest deeper analogies but, at a closer look, the similarity is only formal because in optics the two components of the electric field, E_x and E_y, can be independently modified, unlike the two components of the spinorial wavefunction in graphene. In other words, the chirality of charge carriers in graphene has no classic analog [19].

A simple illustration of this fact is the refraction at the interface between two homogeneous regions in graphene, with constant potential energies V_1 and V_2, the reflection and transmission coefficients in this case being given by

$$r_{gr}=\frac{s_1\exp(i\phi_1)-s_2\exp(i\phi_2)}{s_1\exp(-i\phi_1)+s_2\exp(i\phi_2)},\qquad t_{gr}=\frac{2s_1\cos\phi_1}{s_1\exp(-i\phi_1)+s_2\exp(i\phi_2)} \tag{8}$$

where $\phi_{1,2}$ are the angles between the wavevector and the normal to the interface in the two regions, and $s_{1,2} = sgn(E - V_{1,2})$. Thus, at normal incidence, for $s_1 = s_2$, we obtain $R_{gr} = |r_{gr}|^2 = 0$ and $T_{gr} = (s_2 \cos\phi_2 / s_1 \cos\phi_1)|t_{gr}|^2 = 1$. On the other hand, at normal incidence on an interface separating two materials with refractive indices n_1 and n_2, the corresponding coefficients are

$$r_{opt} = \frac{n_1 - n_2}{n_1 + n_2}, \qquad t_{opt} = \frac{2n_1}{n_1 + n_2} \tag{9}$$

the reflectance $R_{opt} = |r_{opt}|^2$ being different from zero, and the transmittance $T_{opt} = (n_2/n_1)|t_{opt}|^2$ being different from 1. The incident, reflected and transmitted waves in the two situations are denoted by *in*, *r* and *t* in Fig. 2. Unlike in the case of electrons, the reflection and transmission coefficients for light are not generally complex in passive media, so that equations (8) and (9) cannot be similar except when the phases of the incident, reflected and transmitted electromagnetic fields are modified with θ_1, $-\theta_1$ and, respectively, θ_2. Figure 2 illustrates the virtual introduction, which is difficult to implement, of these additional phase factors in the optical case, for normal incidence.

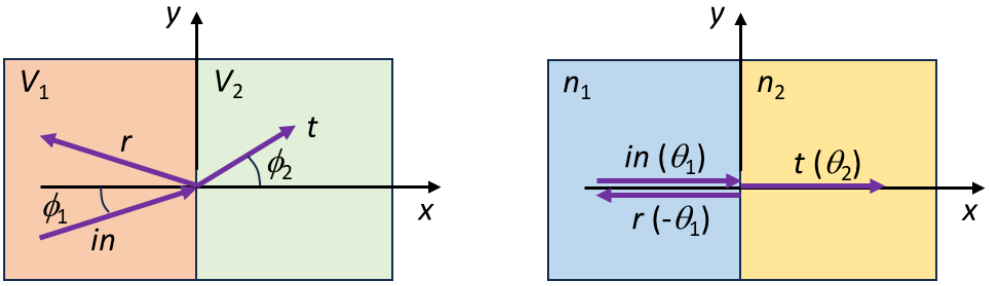

Fig. 2. The refraction of an electron beam at the interface between two regions with different potential energies in graphene (left) can be mimicked in optics (right) only by the introduction of additional phase factors shown in parenthesis.

the reflectance $R_{opt} = |r_{opt}|^2$ being different from zero, and the transmittance $T_{opt} = (n_2/n_1)|t_{opt}|^2$ being different from 1. The incident, reflected and transmitted waves in the two situations are denoted by *in*, *r* and *t* in Fig. 2. Unlike in the case of electrons, the reflection and transmission coefficients for light are not generally complex in passive media, so that equations (8) and (9) cannot be similar except when the phases of the incident, reflected and transmitted electromagnetic fields are modified with θ_1, $-\theta_1$ and, respectively, θ_2. Figure 2 illustrates the virtual introduction, which is difficult to implement, of these additional phase factors in the optical case, for normal incidence.

On the other hand, if in graphene the transmitted spinorial wavefunction can be linked to the incident one via a matrix of the form

$$M = \begin{pmatrix} 1 & 0 \\ 0 & \mathrm{sgn}(s_2/s_1)\exp[\,i(\phi_2-\phi_1)] \end{pmatrix} \tag{10}$$

where $\Psi_t = M\Psi_{in}$, with

$$\Psi_{in} = \frac{1}{\sqrt{2}}\begin{pmatrix} 1 \\ s_1\exp(\,i\phi_1) \end{pmatrix}, \quad \Psi_t = \frac{1}{\sqrt{2}}\begin{pmatrix} 1 \\ s_2\exp(\,i\phi_2) \end{pmatrix}, \tag{11}$$

in optics the corresponding Jones vectors $J_t = M_{ret}J_{in}$ should be connected by a matrix

$$M_{ret} = \begin{pmatrix} 1 & 0 \\ 0 & \exp(\,i\Delta\theta) \end{pmatrix}. \tag{12}$$

which characterizes an optical phase shifter that introduces a phase difference of $\Delta\theta$ between the components of the electric field. This change of the polarization state of the electromagnetic field can be achieved by a birefringent plate [19].

The previous examples suggest that optical structures/systems analogous to nanostructures traversed by ballistic electrons differ depending of the evolution equations obeyed by electrons. However, both light beams and ballistic electrons satisfying the Schrödinger or Dirac equations suffer the same fractional Fourier transform after propagating along a distance L_α through a medium with a refractive index or, respectively, a potential energy that varies gradually along the direction normal to the propagation axis, say y. More precisely, the solution of the equation

$$\left[\left(\frac{\partial^2}{\partial x^2}+\frac{\partial^2}{\partial y^2}\right)+\frac{\omega^2 n^2}{c^2}\right]E(x,y) = 0 \tag{13}$$

satisfied by the electric field in a planar waveguide in which the refractive index varies according to $n(x) = n_0 - n_1x^2/2$ can be expressed as a fractional Fourier transform of order α of the incident electric field. In general this transform of a function ψ can be written as

$$F_\alpha\psi(x') = \sqrt{\frac{exp[\,i(\pi/2-\alpha)]}{2\pi\,sin\,\alpha}}\int \psi(x)\,exp\left(-i\frac{x^2+x'^2}{2\,tan\,\alpha}+i\frac{xx'}{sin\,\alpha}\right)dx \tag{14}$$

the usual Fourier transform being obtained for $\alpha = \pi/2$. The propagation length necessary to generate the Fourier transform in the graded-index waveguides is $L_\alpha = \alpha\sqrt{n_0/n_1}$.

Analogously, for electrons propagating in the ballistic regime through a region in which the potential energy varies as $V(x) = V_0 + \gamma x^2$ the fractional Fourier

transform of the wavefunction of order α is obtained after propagation on a distance $L_\alpha = \alpha\sqrt{(E-V_0)/\gamma}$ for electrons satisfying the Schrödinger equation [20]

$$\left[-\frac{\hbar^2}{2m}\left(\frac{\partial^2}{\partial x^2}+\frac{\partial^2}{\partial y^2}\right)+V(x)-E\right]\Psi=0 \tag{15}$$

and, respectively, after the propagation distance $L_\alpha = \alpha\sqrt{(E-V_0)/2\gamma}$ for Dirac electrons that obey the equation [23]

$$\left[\hbar^2 v_F^2\left(\frac{\partial^2}{\partial x^2}+\frac{\partial^2}{\partial y^2}\right)+(E-V)^2\right]\Psi_{1,2}=0 \tag{16}$$

Potential energies with graded profiles can be induced electrostatically, using curved or segmented gate electrodes. Figure 3 illustrates the trajectory of a beam of light or electrons in a medium with a graded profile of the refractive index or, respectively, of the potential energy.

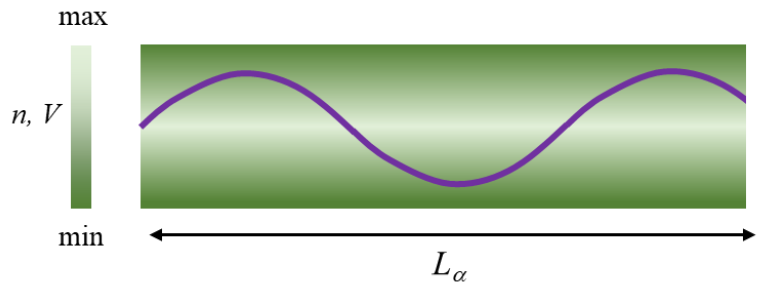

Fig. 3. Schematic representation of the trajectory of a light or electron beam in a medium with a graded profile of the refractive index or, respectively, of the potential energy

3. Quantitative classical optics–ballistic electrons analogies

In the previous section I mentioned some examples of analogies between the propagation of the electromagnetic field and the evolution of electrons in the ballistic regime based on existing similarities between the corresponding equations satisfied by light beams and, respectively, electrons. The Snell law, for instance, already suggests that a succession of layers with different refractive indices modulates the propagation of the electromagnetic field in a similar manner as the action on an electron beam of a succession of regions with different potential energies, all smaller than the energy of ballistic electrons. This similarity, represented schematically in Fig. 4, implies the possibility of finding a more rigorous analogy between optics and ballistic electrons.

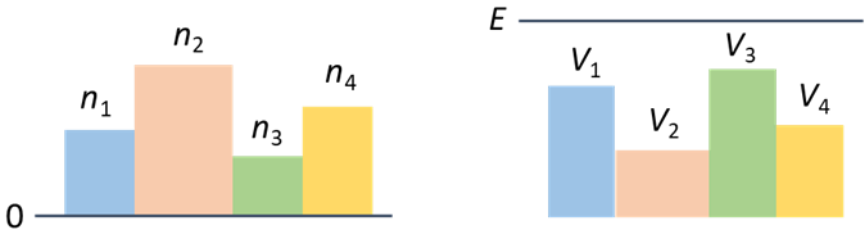

Fig. 4. A succession of layers with different refractive indices (left) modulates an incident electromagnetic field similarly to the action of a succession of regions with different potential energies (right) on the electronic wavefunction.

In this section I will present examples of identifying some quantitative analogies, with the purpose of designing optical systems in which the electromagnetic field in each transverse plane to the propagation direction has the same value as the quantum wavefunction of ballistic electrons in given semiconducting nano-structures. In particular, this requirement imposes the equality of the transmission coefficient and the traversal time (defined in terms of the group velocity) in the corresponding optical and nanoelectronic structures.

This research topics, although apparently superfluous, is motivated both by technological considerations and theoretical opportunities. It is evident that the optical structures are much easier to fabricate and characterize than their analogs in nanoelectronics. In addition, the optical systems can mimic non-standard or difficult to engineer situations/interactions in nanostructures, such as well-defined shapes/boundaries, variable speeds of charge carriers or controllable spin-orbit couplings. Moreover, the propagation of the electromagnetic field in these structures can suggest ways of understanding, respectively, can contribute via measurements in optics to clarify some concepts in quantum mechanics such as the traversal or tunneling time, which is not even defined in quantum theory since no operator is associated to time. Another problem that has no unique solution and can benefit from experiments in classical optics is the transformation of the quantum wavefunction at propagation across an interface separating regions with different evolution equations: Schrödinger versus Dirac [22].

3.1. Quantitative classical optics–Schrödinger electrons analogies

To find such quantitative analogies it is necessary to determine beforehand a set of quantities that vary in similar ways in the equivalent optical and quantum structures. In this respect, besides the already mentioned formal analogies between the vector potential and the scalar wavefunction of electrons satisfying the Schrödinger equation, respectively, between k and □, a similarity condition must be imposed between the group velocities of light and ballistic electrons, defined as [23]

$$v_{go} = 1/\sqrt{\varepsilon\mu} = S/W = |\,\mathrm{Re}[\,(i\omega/\mu)\boldsymbol{A}\cdot\nabla\boldsymbol{A}^*/2]/(\omega^2\varepsilon|\boldsymbol{A}|^2/2) \quad (17a)$$

$$v_g = J/|\Psi|^2 = \mathrm{Re}[\,i\hbar\Psi\cdot\nabla\Psi^*/m]/|\Psi|^2 \quad (17b)$$

In addition, proper boundary conditions need to be specified at an interface, which implies

(i) the continuity of Ψ and $\nabla\Psi\cdot\hat{\boldsymbol{z}}/m$ in quantum mechanics.
In optics, however, the conditions imposed at the interface are different for the two types of light polarization: transverse electric and transverse magnetic, as follows:

(ii) $\boldsymbol{A}$ and $\nabla\boldsymbol{A}\cdot\hat{\boldsymbol{z}}/\mu$ must be continuous in the first case
and

(iii) $(\nabla\times\boldsymbol{A})/\mu$ and $\nabla(\nabla\times\boldsymbol{A})\cdot\hat{\boldsymbol{z}}/\varepsilon\mu$ in the second case,
so that two sets of characteristic parameters of the electromagnetic field can be determined that are similar to those associated to the propagation of the quantum wavefunction, one set for each polarization. More precisely [23],

(i) Ψ, $2(E–V)/\hbar$, m and $1/[2(E–V)]$ are analogous, respectively, with

(ii) $\boldsymbol{A}$, ω, μ and ε for transverse electric waves,

and with

(iii) $(\varepsilon/\mu)^{1/2}\boldsymbol{A}$, ω, ε and μ for transverse magnetic waves.

These quantitative relations between the quantum wavefunction and the linear polarized electric field can be generalized to electromagnetic fields linearly polarized at an arbitrary angle α, seen as an additional degree of freedom for the design of optical structures with specific properties [24].

For exemplification, Fig. 5 illustrates a quantum well in the material mat1 (GaAs), extending in the *x*-*y* plane and defined by the potential barriers of the layers of material mat2 (AlAs), and in which the electrons are incident from, respectively are collected by contacts of mat1 (doped GaAs) situated at the left and, respectively, right side. Ballistic electrons propagate with constant energy E, the potential energies in the quantum well and barriers being denoted as V_w and V_b. From a geometrical point of view, the optical analog has the same configuration, the corresponding layers to the contacts and quantum well, mat1, having a higher refractive index, n_w, and those similar to the potential barriers, mat2, having a lower refractive index, n_b. In this case the electromagnetic with transverse magnetic polarization propagates such as the parameter
$N = k_x c/\omega = n_b sin\theta_b = n_w sin\theta_w$
remains constant, with k_x the wavevector component along the x direction, and θ_b and θ_w the angles between the propagation directions of the electron beam in the quantum barrier and well regions with the normal at the interfaces (z axis). In the

quantum well, assuming ballistic electrons normally incident on interfaces, resonant energy levels can form, denoted in Fig. 5 with E_1 and E_2, for which the transmission of electrons has significant values and the associated traversal time in nanostructures shows sharp minima.

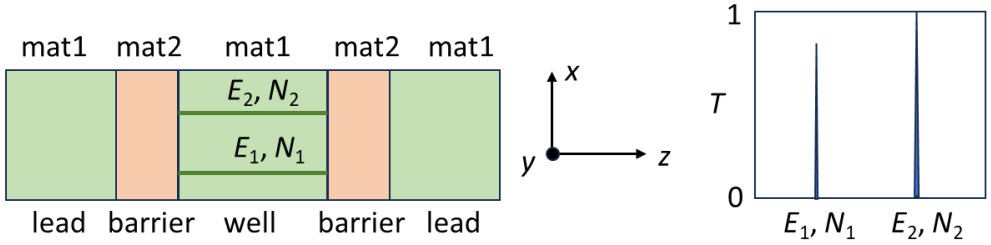

Fig. 5. Schematic representation of a quantum well for electrons (respectively of the corresponding optical structure), and of the resonant energy levels for E (for the propagation constant N) (left). Transmission variation for the resonant values of E, respectively N (right).

To obtain a quantitative optical analog of the quantum well it is necessary to establish how N and the frequency ω depend on the parameters of the two structures (quantum and optical), and to find the dimensions of the layers with higher and lower refractive indices, which correspond to the potential wells and barriers for electrons. If the analogies mentioned above are sufficient to fulfill the first condition, leading to the following expressions of the dependence on the electron energy of N:

$$N^2 = \frac{n_b^2(E - V_w) + an_w^2(V_b - E)}{(E - V_w) + a(V_b - E)} \tag{18}$$

with $a = n_b^4 m_w / n_w^4 m_b$, respectively of the relation of the optical frequency on N:

$$\omega(N) = \omega_0 \sqrt{\frac{n_w^2 - n_b^2}{(N^2 - n_b^2) + a(n_w^2 - N^2)}}, \quad \omega(V_w) = \omega_0 \tag{19}$$

to find the dimensions of the layers with different refractive indices an additional requirement should be imposed: the phases acquired by the electromagnetic field and the quantum wavefunction in the corresponding layers should be equal. Then, for a quantum well in GaAs/AlAs with thicknesses of the barriers and well of some tens of Ångstroms, the respective thicknesses of the layers with different refractive indices are of the order of tens of microns for $\omega_0 = 1$ μm, the optical structures being much easier to fabricate and measure [25]. This example emphasizes the fact that to obtain the same values of the electromagnetic field at different interfaces, respectively the same transmission coefficient and traversal time as the corresponding values of the wavefunction, transmission coefficient and traversal time in terms of E, it is necessary that the frequency and incidence angle of the optical beam vary simultaneously.

Similar results can be obtained for the quantitative optical analog of a quantum wire, which has a geometry like that in Fig. 5, except that the dimension of the nanostructure along the y direction is restricted to a value L. In this situation, due to the confinement of the wavefunction along y, the minimum energies of electrons in the potential barrier and well regions are

$E_w = V_w + (p\pi\hbar/L\sqrt{2m_w})^2$, $E_b = V_b + (p\pi\hbar/L\sqrt{2m_b})^2$

with p an integer. Also in this case the thicknesses of the layers with different refractive indices, n_w and n_b, for $L = L_w = L_b = 100$ Å are of the order of microns, their actual values depending on p/on the transverse mode [26]. In this example, again, a variation of the energy of ballistic electrons in the quantum wire is equivalent with a simultaneous variation of N and ω in the optical case, for the resonant states the transmission coefficient being maximum and the traversal time minimum. Similarly, optical structures can be found that are quantitative analogs of quantum wires with a constant potential energy but inhomogeneous cross-section, characterized by minima of the transmission coefficient and maxima of the traversal time for resonant states [26].

Finally, quantitative optical analogs can be identified for quantum dots with either constant cross-section but variable potential energy or constant potential energy but variable cross-section [27]. These structures have similar dependences of the transmission coefficient and traversal time as a function of E for electrons, or as a function of N for light beams. However, besides the variation of N and ω in terms of E, to find the dimensions of optical structures corresponding to quantum dots, the requirement of phase equality at propagation through corresponding layers is no longer sufficient, the introduction of additional phases being needed. These examples illustrate the fact that the design of quantitative analogous structures to nanostructures for ballistic electrons is not trivial but implies a constructive use of classic-quantum analogies.

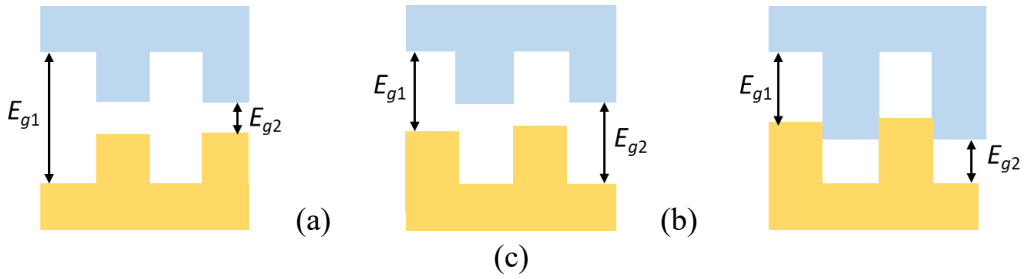

Fig. 6. Schematic representation of the conduction and valence bands in heterostructures of type I (a), II (b) and III (c).

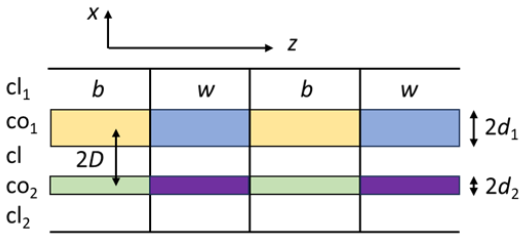

Fig. 7. System of two coupled waveguides analogous to heterostructures of type II and III.

Nanoelectronic devices are generally based on type I heterostructures, as those in Fig. 6(a), in which the transport of electrons in the conduction band and of holes in the valence band across a succession of layers acting as potential barriers or wells can be described independently. This situation is, however, not always justifiable. In type II or III heterostructures, as those illustrated in Figs. 6(b) and, respectively, 6(c), the wavefunctions associated to charge carriers in the conduction (subscript *c*) and valence bands (subscript *v*) are coupled:

$$-i\frac{d}{dz}\begin{pmatrix}\Psi_c\\ \Psi_v\end{pmatrix}=\begin{pmatrix}0 & \dfrac{E-E_v}{\hbar P}\\ \dfrac{E-E_c}{\hbar P} & 0\end{pmatrix}\begin{pmatrix}\Psi_c\\ \Psi_v\end{pmatrix} \tag{20}$$

where the parameter P is related to the effective mass of carriers as $m=(m_0^{-1}+2P^2/E_g)^{-1}$ and the group velocity is given by

$$v_g = J/\varrho = P(\Psi_c\Psi_v^* + \Psi_v\Psi_c^*)/(|\Psi_c|^2+|\Psi_v|^2). \tag{21}$$

Do quantitative optical analogies exist in this case also? A possible optical structure that meets this challenge is a hybrid between a directional coupler and a Bragg reflector, which consists from two very dissimilar (with very different diameters d_1 and d_2) coupled waveguides, which allow the propagation of only two coupled modes with amplitudes $\boldsymbol{e}_{1,2}$ and propagation constants $\beta_{1,2}$, such that the total electric field is $E=a_1\boldsymbol{e}_1\exp(i\beta_1 z)+a_2\boldsymbol{e}_2\exp(i\beta_2 z)$. This structure, represented in Fig. 7, is the only one in which the co-propagating modes are coupled and the reflection and transmission coefficients are nontrivial, since it is formed from a succession of different regions. Such structures can eventually be implemented in integrated optics.

With the change of variables $b_i(z)=a_i(z)\exp[-i(\beta_1+\beta_2)z/2]$, the system of coupled equations that these modes satisfy can be written as

$$-i\frac{d}{dz}\begin{pmatrix}b_1\\ b_2\end{pmatrix}=\begin{pmatrix}\Delta\beta & C_{12}\\ C_{21} & -\Delta\beta\end{pmatrix}\begin{pmatrix}b_1\\ b_2\end{pmatrix} \tag{22}$$

Equations (20) and (22) are similar if $\Delta\beta=(\beta_1-\beta_2)/2\equiv 0$ and $C_{12}\neq C_{21}$, where the coupling coefficients are $C_{nm}=(k/4)\sqrt{\varepsilon_0/\mu_0}\int_A(n^2-n_n^2)\boldsymbol{e}_n^*\boldsymbol{e}_m dA$, n,m =

1,2. Starting from the systems of equations (20) and (22), we find that in order for the quantum wavefunctions in heterostructures to have the same forms at interfaces as the electromagnetic field in the coupled waveguides, the conditions that must be fulfilled are

$$L_j k_j = L_{jo}\gamma_j\beta_j/\sqrt{\beta_j^2 - N^2} \text{ and } \sqrt{(E-E_{cj})/(E-E_{vj})} = \sqrt{C_{21j}/C_{12j}} \qquad (23)$$

with L_j, L_{jo} the lengths of the regions corresponding to wells and barriers for electrons and, respectively, their optical analogs, $k_j = \sqrt{(E-E_{vj})(E-E_{cj})}/\hbar P_j$, $N = \beta_j \sin\theta_j$, and $\gamma_j = \sqrt{C_{12j}C_{21j}}$, j = w,b. These conditions impose a certain dependence between the parameters of the optical system and the energy of charge carriers in heterostructures [28].

Another example of quantitative analogies between classical optics and Schrödinger electrons that propagate in the ballistic regime involves nanostructures in which spin-orbit coupling exists, for instance those in which electrons are subject to the Rashba effect. The total Hamiltonian of the system of charge carriers in the presence of this effect can be written as

$$H = \frac{\hbar^2 k^2}{2m} + H_R = \begin{pmatrix} (\hbar^2 k^2)/2m + \alpha k_x & -\alpha k_z \\ -\alpha k_z & (\hbar^2 k^2)/2m - \alpha k_x \end{pmatrix} \qquad (24)$$

where α is the Rashba coefficient, the two solutions for the propagation vectors at constant energy of electrons incidents at the interface between a conductor in which the effect is absent and another in which it exists being

$$k_{\pm}^R = \frac{m}{\hbar^2}\left(\sqrt{\alpha^2 + 2\hbar^2 E/m} \mp \alpha\right), \qquad (25)$$

while the propagation angles with respect to the normal at the interface are $\varphi_{\pm}^R = arcsin(k_z/k_{\pm}^R)$. Thus, the splitting of the electron beam in two beams, with corresponding orthogonal wavefunctions:

$$\begin{aligned} \psi_+^R &= exp(ik_{+x}^R x + ik_z z)\begin{pmatrix} cos(\varphi_+^R/2) \\ -sin(\varphi_+^R/2) \end{pmatrix}\psi_-^R \\ &= exp(ik_{-x}^R x + ik_z z)\begin{pmatrix} sin(\varphi_-^R/2) \\ cos(\varphi_-^R/2) \end{pmatrix} \end{aligned} \qquad (26)$$

is similar to the double refraction of light in a birefringent crystal, in which the two resulting beams have orthogonal polarizations. Figure 8 illustrates this analogy. By denoting with δ_i the incidence angle of an optical beam on the interface between an isotropic crystal and an uniaxial one, and with δ_e and δ_o the corresponding angles of the resulting extraordinary and ordinary beams with respect to the normal at the interface, a quantitative analogy between the propagation of ballistic electrons and the electromagnetic field implies the identification, for a birefringent crystal with given ordinary and extraordinary refractive indices, of the angle δ_i such that $\varphi_-^R =$

δ_o or $\varphi_+^R = \delta_o$. Numerical investigations of this problem for an uniaxial BBO crystal were reported in Ref. [29] for different values of the Rashba coefficient, and the energy and incidence angle of electrons, in each case the corresponding angles δ_1, δ_o and δ_e being determined. In a similar manner one can find the optical analog of a nanostructure with Dresselhaus effect, or in the simultaneous presence of Rashba and Dresselhaus effects.

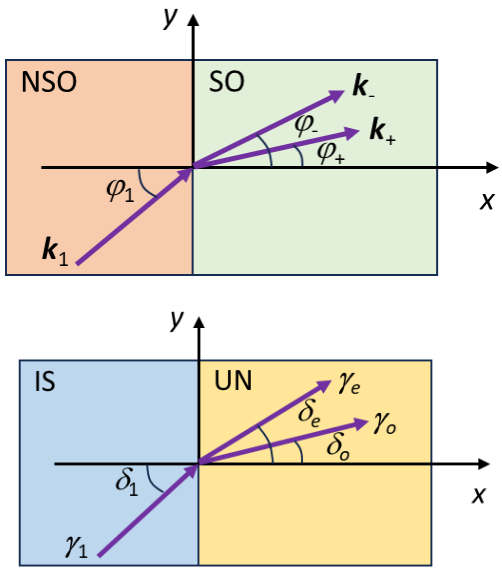

Fig. 8. The splitting of an electron beam at the interface between a material with no spin-orbit coupling (NSO) and another in which this coupling exist (SO) is analogous to the double refraction of an optical beam at the interface between an isotropic material (IS) and a birefringent, uniaxial (UN) one.

Regarding the quantitative analogy classical optics–Schrödinger electrons, the opposite situation, in which nanostructures for ballistic electrons can be designed starting from optical systems, exists also. In particular, a nanostructure was found in which the charge carriers propagate similarly to the electromagnetic field in a metamaterial with negative refractive index. This similarity is based on the formal analogy between Maxwell's equations for monochromatic plane waves and the Schrödinger equation written in the matrix form:

$$\frac{d}{dz}\begin{pmatrix} E_y \\ iH_x \end{pmatrix} = \begin{pmatrix} 0 & \omega\mu \\ -\omega\varepsilon & 0 \end{pmatrix}\begin{pmatrix} E_y \\ iH_x \end{pmatrix}, \quad \frac{d}{dz}\begin{pmatrix} \Psi \\ \Phi \end{pmatrix} = \begin{pmatrix} 0 & \hbar/m \\ 2(V-E)/\hbar & 0 \end{pmatrix}\begin{pmatrix} \Psi \\ \Phi \end{pmatrix} \qquad (27)$$

with $(\hbar/m)\Phi = d\Psi/dz$. From (27) it follows that a material with $\varepsilon < 0$, $\mu < 0$ is equivalent with one in which the effective mass of electrons is negative: $m < 0$ and their energy is smaller than the potential energy: $E < V$, i.e., with a potential barrier

for carriers with $m < 0$. In particular, semiconductors like GaN, AlN, $In_{0.53}Ga_{0.47}As$, InAs, or InP have negative effective mass values along some crystallographic directions [30]. As such, it is feasible to find a quantitative analog for optical metamaterials in the sense specified above. Indeed, for a nanostructure in which one metamaterial with $m < 0$ and $E < V$ is placed between two materials with $m > 0$ and $E > V$, a computation of the traversal time defined in terms of the group velocity showed that for small values of the electron energy the analog of the optical metamaterial accelerates the ballistic electrons compared with the situation in which this layer does not exist, similarly with superluminal propagation of electromagnetic waves, while for higher electron energy values (but still smaller than V), the ballistic electrons are slowed down, similarly with the subluminal propagation of optical beams (slow light) [31]. It becomes thus possible to modulate the traversal time of a nanostructure by modifying the energy of the incident electrons.

3.2. Quantitative classical optics– Dirac electrons analogies

Because photons have a linear dispersion relations, similar to that of Dirac-like electrons in graphene, it is expected that quantitative analogies are easier to find in this case. The reality is different, however, such analogies being identified only between ballistic electrons and complex conjugate optical media [32]. The latter are materials with complex relative electric permittivity and relative magnetic permeability, but a real refractive index:

$$\varepsilon_r = m(a + ib),\ \mu_r = a - ib,\ n = \sqrt{\varepsilon_r \mu_r} = \sqrt{m(a^2 + b^2)} \tag{28}$$

and which under certain circumstances can act as active lasing media that do not require a resonant cavity for the emission of coherent radiation. These are the only materials with complex transmission (and reflection) coefficient for optical beams incident under an angle θ_1 from air (the propagation angle in the complex conjugate medium is θ_2):

$$t_{ccm} = 2\frac{(a-ib)\cos\theta_1}{(a-ib)\cos\theta_1 + \sqrt{m(a^2+b^2)}\cos\theta_2}, \tag{29}$$

similar to the complex transmission coefficient of the wavefunction in graphene at the interface between two regions with different potential energies, in which ballistic electrons propagate at angles ϕ_1 and ϕ_2 with respect to the normal at the interface, as in Fig. 2. The corresponding expression of the transmission coefficient in graphene is given in equation (8). The equality of the transmission coefficients in optics and for electrons requires that the following conditions are simultaneous satisfied:

$$\frac{cos\phi_1 + cos\phi_2}{sin\phi_1 - sin\phi_2} = \frac{Re[t_{ccm}]}{Im[t_{ccm}]},\ \ \frac{cos\phi_1(sin\phi_1 - sin\phi_2)}{1+\cos(\phi_1+\phi_2)} = Im[t_{ccm}]; \tag{30}$$

these conditions can be fulfilled for certain values of m, a and b, in the sense that corresponding incidence angles on the complex conjugate medium can be found for given values of ϕ_1 [33].

On the other hand, a quantitative analogy between the transmission probability of electrons in graphene and the transmittance of normally incident optical beams at the interface between two media with different but real refractive indices (passive optical media) is possible only in relatively narrow ranges of the parameters involved. Such ranges were identified for quantitative analog structures of a simple interface, a layer with finite thickness, and, respectively, a periodic structure for both light and electron beams [34].

4. Apparent analogies

Although in the examples of classical optics–ballistic electrons analogies presented above the optical structures/systems and the quantum nanostructures had similar configurations, a corresponding scaling of an optical system may not always produce the desired effect on ballistic electrons. The reason is that, besides the similar evolution laws of optical or electron beams, there are other considerations that must be accounted for in order for an analogy to work, such as the specific excitation mode of surface plasmon polaritons, for example. Nevertheless, the working principle of a plasmonic system can be used to inspire an equivalent electron optic system.

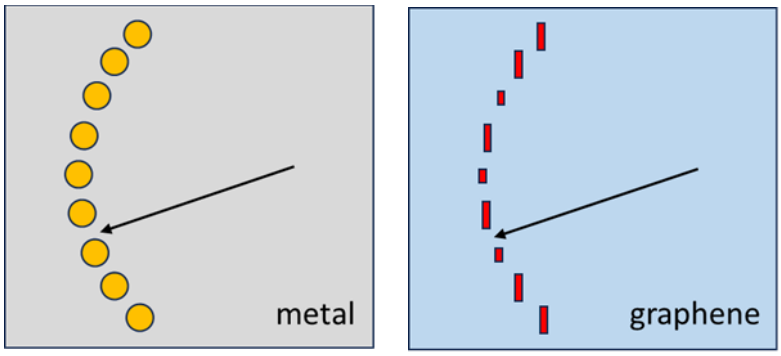

Fig. 9. Schematic representation of an array of circular holes in metal that works as a plasmonic lens (left) and a similar array of nanopores which, under certain circumstances, focalizes an electron beam in graphene (right).

To illustrate this analogy, Fig. 9 presents an array of holes in a metallic surface, which form an arc of a circle and focalizes the electromagnetic field of the surface plasmon polaritons propagating at the air/metal interface [35]. The working principle is based on the constructive interference of light excited by each hole. According to the examples of analogies between classical optics and ballistic

electrons mentioned in the previous sections, a similar configuration of potential barriers, for instance nanopores in graphene, should produce a similar effect. However, numerical simulations for electrons propagating in the ballistic regime in a graphene ribbon with circular nanopores with dimensions scaled appropriately and passivated with hydrogen atoms showed that the circular nanopore array acts as an impregnable potential barrier that scatters the incident electron beam instead of focalizing it. This result highlights the fact that not only similarities but also differences exist between the propagation of light and of ballistic electrons. More precisely, a simple scaling of the plasmonic lens in optics does not account for the fact that the holes in metal do not only induce the phase factors necessary for focalization but are essential also for the excitation of surface plasmon polaritons, role with no correspondence in the case of ballistic electrons.

However, the working principle of the plasmonic lens can still be used to focalize ballistic electrons if the nanopores have smaller dimensions along their propagation direction, such that the incident electrons can tunnel with high probability through the potential barriers associated to the nanopores. After performing a large number of numerical simulations, we found an optimum configuration of rectangular nanopores, with different dimensions put still placed on an arc of a circle, which can focalize or anti-focalize an incident electron beam depending on the passivation of the nanopores' edges [36]. More precisely, we have considered nanopores with armchair edges along the propagation direction of the electron beam, passivated with one hydrogen atom, and zigzag edges along the transverse direction. The latter can be passivated with one or two hydrogen atoms, depending on the geometry of the nanopore and the chemical potential of hydrogen [37]. The focalization of ballistic electrons is obtained when the nanopores are passivated with a single hydrogen atom, the system of nanopores being equivalent with a meniscus in optics, and the focal distance depends on the electron energy, as follows from the Snell law in (4). On the other hand, the nanopores passivated with two hydrogen atoms anti-focalize the beam of electrons, phenomenon with no counterpart in optics and which involves the emergence of a region with a lower probability of finding electrons than the surrounding areas. Both focalization and anti-focalization of ballistic electrons in graphene ribbons with nanopores placed along an arc of a circle occur only in the energy range of electrons in which a single transverse mode is able to propagate in the nanoribbon.

Conclusions

The analogies between classical optics and ballistic electrons, irrespective of the equation that these satisfy (Schrödinger or Dirac), led to the development of devices/systems with practical applications and/or to changing perspectives on investigations of fundamental concepts in quantum mechanics. In the vast majority

of cases optical structures analogous to some quantum nanostructures or vice-versa are obtain by an appropriate scaling of their dimensions. In addition, if the development of quantitative analogies is required, in which the wavefunction and, respectively, the electromagnetic field propagate in similar manners through equivalent structures, such that the transmission coefficients and the traversal time are identical, sets of corresponding parameters in optics and for electrons can most often be found. On the other hand, the identification of classical optics–ballistic electrons analogies is not a trivial task. For such analogies to work, not only the respective evolution equations and the relevant boundary conditions but also the excitation of the involved beams must be taken into consideration. It is important to emphasize that not only similarities but also differences exist between the propagation of optical and electronic beams. To highlight them and, moreover, to transform these differences in inspiration sources for unexpected analogies is perhaps one of the most interesting challenges for future research in this direction.

REFERENCES

[1] E. Ruska, Z. Phys. **87**, 580 (1934).
[2] G.N. Henderson and T.K. Gaylord, E.N. Glytsis, Proc. IEEE **79**, 1643 (1991).
[3] G.N. Henderson and T.K. Gaylord, E.N. Glytsis, J. Opt. Soc. Am. B **10**, 333 (1993).
[4] J. Spector *et al*., Appl. Phys. Lett. **56**, 2433 (1990).
[5] J. Spector *et al*., Appl. Phys. Lett. **56**, 1290 (1990).
[6] C. Bauerle et al., Rep. Prog. Phys. **81**, 056503 (2018).
[7] J.D. Joannopoulos *et al*., *Photonic Crystals: Molding the Flow of Light* (Princeton Univ. Press, Princeton, 2008) 2nd edition.
[8] A.S.L. Gomes *et al*., Prog. Quantum Electron. **78**, 100343 (2021).
[9] D. Spirito *et al*., Phys. Rev. B **85**, 235314 (2012).
[10] A.H. Castro Neto *et al*., Rev. Mod. Phys. **81**, 109 (2009).
[11] V.V. Cheianov *et al*., Science **315**, 1252 (2007).
[12] S. Chen *et al*., Science **353**, 1522 (2016).
[13] C. Déprez *et al*., Nature Nanotechnol. **16**, 555 (2021).
[14] S. Bittner *et al*., Phys. Rev. B **82**, 014301 (2010).
[15] D. Dragoman and M. Dragoman, Solid-State Electron. **211**, 108818 (2024).
[16] H. Luo *et al*., Opt. Commun. **254**, 353-360 (2005).
[17] S.K. Mishra *et al*., J. Phys.: Condens. Matter **9**, 461 (1997).
[18] A. Radu *et al*., J. Appl. Phys. **112**, 024318 (2012).
[19] D. Dragoman, J. Opt. Soc. Am. B **27**, 1325 (2010).
[20] D. Dragoman and M. Dragoman, J. Appl. Phys. **94**, 4131 (2003).
[21] D. Dragoman, Beilstein J. Nanotechnol. **9**, 1828 (2018).
[22] D. Dragoman, J. Appl. Phys. **113**, 214312 (2013).
[23] D. Dragoman and M. Dragoman, Prog. Quantum Electron. **23**, 131 (1999).
[24] D. Dragoman, J. Opt. Soc. Am. B **29**, 1528 (2012).
[25] D. Dragoman and M. Dragoman, Opt. Commun. **133**, 129 (1997).
[26] D. Dragoman and M. Dragoman, IEEE J. Quantum Electron. **33**, 375 (1997).
[27] D. Dragoman and M. Dragoman, Opt. Commun. **150**, 331 (1998).

[28] D. Dragoman, J. Appl. Phys. **88**, 1 (2000).
[29] D. Dragoman, J. Opt. **16**, 015710 (2014).
[30] Z.S. Gribnikov *et al*., IEEE J. Sel. Top. Quantum Electron. **7**, 630 (2001).
[31] D. Dragoman and M. Dragoman, J. Appl. Phys. **101**, 104316 (2007).
[32] D. Dragoman, Opt. Commun. **284**, 2095 (2011).
[33] D. Dragoman *et al*., J. Opt. **15**, 035710 (2013).
[34] Mihalache and D. Dragoman, J. Opt. Soc. Am. B **28**, 1746 (2011).
[35] L. Yin *et al*., Nano Lett. **5**, 1399 (2005).
[36] D. Mladenovic and D. Dragoman, Nanomaterials **12**, 529 (2022).
[37] T. Wassmann *et al*., Phys. Rev. Lett. **101**, 096402 (2008).